NASA TECHNICAL MEMORANDUM

NASA TM X-72837

NASA TM X-72837

COMPARISON OF SUPERCRITICAL AND CONVENTIONAL WING FLUTTER CHARACTERISTICS

By Moses G. Farmer, Perry W. Hanson and Eleanor C. Wynne

(NASA-TM-X-72837) COMPARISON OF SUPERCRITICAL AND CONVENTIONAL WING FLUTTER CHARACTERISTICS (NASA) 9 p HC $3.50 N76-22159

CSCL 01A Unclas
G3/02 26794

NATIONAL AERONAUTICS AND SPACE ADMINISTRATION
LANGLEY RESEARCH CENTER, HAMPTON, VIRGINIA 23665

1. Report No.	2. Government Accession No.	3. Recipient's Catalog No.
TMX 72837		

4. Title and Subtitle	5. Report Date
Comparison of Supercritical and Conventional Wing Flutter Characteristics	May 1976
	6. Performing Organization Code: 2711
7. Author(s): Moses G. Farmer, Perry W. Hanson, and Eleanor C. Wynne	8. Performing Organization Report No.
	10. Work Unit No.: 505-02-21-01
9. Performing Organization Name and Address: NASA Langley Research Center, Hampton, VA 23665	11. Contract or Grant No.
	13. Type of Report and Period Covered: Technical Memorandum
12. Sponsoring Agency Name and Address: National Aeronautics & Space Administration, Washington, DC 20546	14. Sponsoring Agency Code

15. Supplementary Notes

Technical Paper Proposed for Presentation at the AIAA/ASME/SAE 17th Structures, Structural Dynamics, and Materials Conference; Valley Forge, PA, May 5-7, 1976

16. Abstract

To evaluate the concern that the flutter characteristics of supercritical wings might be significantly different from those of wings with conventional airfoils, a wind-tunnel study was undertaken to directly compare the measured flutter boundaries of two dynamically similar aeroelastic models which had the same planform, maximum thickness-to-chord ratio, and as nearly identical stiffness and mass distributions as possible, with one wing having a supercritical airfoil and the other a conventional airfoil. The considerations and problems associated with flutter testing supercritical wing models at or near design lift coefficients are discussed, and the measured transonic boundaries of the two wings are compared with boundaries calculated with a subsonic lifting surface theory.

17. Key Words (Suggested by Author(s)) (STAR category underlined)	18. Distribution Statement
Flutter Transonic speeds Airfoil effects	Unclassified - Unlimited

19. Security Classif. (of this report)	20. Security Classif. (of this page)	21. No. of Pages	22. Price*
Unclassified	Unclassified	7	$3.25

*Available from { The National Technical Information Service, Springfield, Virginia 22151
STIF/NASA Scientific and Technical Information Facility, P.O. Box 33, College Park, MD 20740

COMPARISON OF SUPERCRITICAL AND CONVENTIONAL WING FLUTTER CHARACTERISTICS

Abstract

To evaluate the concern that the flutter characteristics of supercritical wings might be significantly different from those of wings with conventional airfoils, a wind-tunnel study was undertaken to directly compare the measured flutter boundaries of two dynamically similar aeroelastic models which had the same planform, maximum thickness-to-chord ratio, and as nearly identical stiffness and mass distributions as possible, with one wing having a supercritical airfoil and the other a conventional airfoil. The considerations and problems associated with flutter testing supercritical wing models at or near design lift coefficients are discussed and the measured transonic boundaries of the two wings are compared with boundaries calculated with a subsonic lifting surface theory.

Introduction

The supercritical wing concept holds much promise for increased aerodynamic efficiency and for allowing more efficient structural design. Of some concern to an aeroelastician is the possibility that wings with supercritical airfoil sections exhibit aerodynamic characteristics substantially different from those of wings with conventional airfoils. Reference 1 presents a good discussion of the different aerodynamic characteristics of supercritical and conventional airfoils. Figure 1 from Reference 1 indicates schematically some of the aerodynamic differences. For instance, in addition to the delayed rise in drag as sonic speed is approached, higher lift coefficients are attainable, the center of pressure is generally located farther downstream, and the pressure distribution may be more sensitive to perturbations in the airfoil shape. There has been, therefore, some concern that the flutter characteristics of such a wing might be significantly different from those of wings with conventional airfoils, and that special model flutter testing techniques, such as testing at or near the design lift coefficient, might be required. This paper presents some results of a study that was undertaken to evaluate this concern, to determine unique problems, if any, associated with wind-tunnel testing of supercritical wing flutter models, and to evaluate the suitability of a typical current transonic flutter analysis procedure for supercritical wings.

Modeling and Testing Considerations

Approach

The approach selected was to directly compare the measured flutter characteristics of two dynamically similar transonic aeroelastic models which had the same planform, maximum thickness-to-chord ratio and as nearly identical stiffness and mass distributions as possible. One had a supercritical airfoil and the other a conventional airfoil. The configuration chosen for the supercritical wing model was that of the research wing on the modified TF-8A airplane, shown in Figure 2 (Ref. 1), which was used as a test bed to evaluate under full-scale conditions the aerodynamic performance predicted by wind-tunnel studies. It was convenient to use this wing configuration because the geometry, including airfoil sections, were already defined and experimental pressure distribution data were available. The wing geometry simulated that which would be applicable to a high-speed transport aircraft but structurally the TF-8A supercritical wing was "boilerplate" in the sense that it was relatively much more stiff (to minimize contour distortions) than a transport wing structure. Therefore, in order to have a model wing with stiffness levels more nearly like a transport wing and to permit flutter speeds attainable in the wind tunnel, the stiffness and mass levels used for the flutter model were considerably reduced from those of the TF-8A research wing although the distributions of stiffness and mass of the model were similar to those of the full-scale wing.

Model Design Considerations

Since there were, at the time of the model design, tentative plans to build a more realistically flexible supercritical wing for the TF-8A airplane for later studies of aeroelastic effects, it was decided to design the model for the present studies so that associated components (i.e., sidewall half-body, balance, etc.) could be used for future flutter clearance and correlation studies for flight/wind-tunnel aeroelastic deformation. These considerations led to a half-body representation of the TF-8A fuselage for tunnel wall mounting the wing, and a geometric scale factor of 0.27. The 0.27-scale factor permits simultaneous Froude number scaling (for static deflections), and Mach number scaling, when the model is tested in Freon in the Langley Research Center Transonic Dynamics Tunnel (TDT) at simulated flight cruise altitudes. In addition, of course, the large scale increases the model Reynolds number, which for these tests varied from about 3 to 9 million, based on the streamwise chord at the two-thirds semispan station. Figure 3 is a photograph of the supercritical wing model mounted in the TDT on the TF-8A half-fuselage. Note that the airplane engine air inlet at the bottom of the fuselage under the cockpit has been faired into the nose contour. No empennage was simulated other than including an equivalent cross-sectional area near the rear of the fuselage.

The companion "conventional" wing model was geometrically identical to the supercritical wing model at the root thus allowing proper fairing into the fuselage half-body. On the conventional wing, airfoil sections derived from those of a current wide-body jet transport were used from the wing tip to 24-percent semispan. Airfoil sections from this location inboard were generated by tangentially

fairing constant percent chord lines between the root airfoil surface (common to both models) and the airfoil surface at the 24% semispan station. Figure 4 is a schematic drawing showing the planform and size of the two model wings and their relationship to the half-body and sidewall mount.

The wings were mounted on a force balance in the fuselage half-body. The balance was attached to a tunnel sidewall turntable which could be rotated to change the wing and half-body angle of attack. The balance measured only static forces on the wing. Electrical resistance wire strain gages mounted on the wings were used to record model motions.

Model Properties

The construction techniques used for both wings were identical. The wings, one of which is shown in Figure 5 before the lower skin was applied, were fabricated with continuous fiberglass skins to provide the smooth surface desirable for supercritical flow. The fiberglass skins, which provided the required design stiffness distributions for the wings, were stabilized with a full depth phenolic impregnated nylon honeycomb core. Ballasting masses were inserted in the core to obtain the desired mass distributions. The masses of the supercritical and conventional wings were 21.205 kg (46.75 lbm) and 21.546 kg (47.50 lbm), respectively. The measured bending and torsion stiffness distributions of the two wings are compared in Figure 6, and the first four measured natural frequencies generalized masses, and node lines of the conventional and supercritical wings are compared in Figure 7. The generalized masses are based on mode shapes normalized to unity at the point of maximum measured modal deflection for each mode. The structural properties of the two wings are seen to be quite similar.

Since the supercritical and conventional wings experience different aerodynamic load distributions, it was desirable to design each wing individually to a "no-wind jig shape" such that at a particular tunnel Mach number and dynamic pressure, each wing deforms under 1-g aerodynamic loads in a manner so that the deflections of the leading and trailing edges of the conventional wing are approximately the same as those of the supercritical wing. This "shape" can be considered the "cruise shape" and the tunnel Mach number and dynamic pressure "cruise conditions." The simulated design tunnel cruise conditions chosen for the two wings were:

	Conventional	Supercritical
Mach Number	0.90	0.99
Dynamic Pressure	2.73 kn/m^2 (57 lbf/sq/ft)	2.20 kn/m^2 (46 lbf/sq/ft)
Lift Coefficient	0.30	0.37
Lift	769N(173 lbf)	769(173 lbf)

The no-wind jig shapes of the conventional and supercritical wings are shown in Figure 8 in terms of the spanwise deviation of the elastic axis (essentially the 50% chord line) from a reference point at the wing root. Also shown is the twist angle measured near the tip.

Wind Tunnel and Test Procedure

The models were tested in the Langley Research Center Transonic Dynamics Tunnel. This tunnel has a 4.88-meter (16-ft) square test section with cropped corners and is a return-flow, variable-pressure, slotted-throat wind tunnel. It is capable of operation at stagnation pressures from about 1724 N/m^2 (1/4 lb/in^2) to atmospheric pressure and at Mach numbers up to 1.2. Mach number and dynamic pressure can be varied independently with either air or Freon-12 used as a test medium. Freon-12 was used in the present investigation. Average stagnation temperature during the tests was approximately 49° C (120° F). In addition to the model instrumentation mentioned previously, motion-picture and still cameras were used to record model dynamic motions and static deflections.

In order to realistically simulate wing deformation due to 1-g lift, the model angle of attack was adjusted to maintain a reasonably constant load of 769 Newtons (173 lbf) (the design lift condition) while searching for the flutter boundaries. Figure 9 illustrates the manner in which the tests were generally conducted. The open symbol indicates the point at which the conventional wing should be deformed to the "cruise shape." (Rough measurements indicated that the cruise shapes of the two wings actually were not precisely the same. This may have been due to slight differences in stiffness or to inaccuracies in calculated aerodynamic loads used to define the jig shapes.) If this point is considered to be the tunnel condition which simulates a transport airplane "cruise" velocity and altitude, then the corresponding required 1.2 V_D flutter safety margin (typically) would be as indicated. Assuming the airplane wing stiffness is properly simulated, then the model wings would progressively deform as would those of a constant weight airplane as the flutter boundary is approached. At flutter onset, fast-acting tunnel bypass valves were opened which rapidly reduced Mach number and dynamic pressure before model damage occurred.

Discussion and Results

Flutter Calculations

Flutter calculations for both the supercritical and conventional wings have been made using measured mode shapes and generalized masses of the first six structural modes. Downwash collocation points were specified at 10 spanwise stations with six points along the streamwise chord at each station. These calculations, which employed subsonic lifting surface theory (Ref. 2) in computer programs that are partially described in Reference 3, made no allowance for airfoil shape since the lifting surface is modeled as a flat plate. Differences in calculated flutter characteristics of the supercritical and conventional wings are therefore attributable only to the structural differences between the wings as reflected in the natural vibration characteristics.

Calculated dynamic pressures at flutter and flutter frequencies are shown in Figure 10 for Mach numbers from 0.6 to 0.99. The calculated dynamic pressure at flutter for the conventional wing (Fig. 10(a)) was consistently lower than that of the supercritical wing throughout the Mach number range. Since subsonic kernel function aerodynamics were used, the results at Mach numbers near one are not

reliable and can only be used to make relative comparisons between the two wings.

The calculated flutter frequencies shown in Figure 10(b) are between the frequencies of the first two structural modes (see Fig. 7). From V-g plots (velocity versus damping) it could be seen that the second bending mode damping became negative at the flutter point.

Values of the mass ratio, μ (ratio of the mass of the wing to the mass of test medium contained in the volume generated by revolving each streamwise chord about its midpoint), at flutter varied from about 8 at 0.6 Mach number up to approximately 30 at 0.99 Mach number.

Wind-Tunnel Results

Measured dynamic pressures at flutter and flutter frequencies for the supercritical and the conventional wing are shown in Figures 11 and 12, respectively. Curves from the calculated results in Figure 10 are shown again for comparison with the experimental results. Qualitatively, the flutter characteristics of the two wings were quite similar. Figures 11(a) and 12(a) indicate that below 0.8 Mach number the calculated and measured dynamic pressures are in fairly good agreement, with the measured values being slightly greater. Above 0.8 Mach number the measured dynamic pressures decrease rapidly with Mach number to a minimum between 1.00 and 1.05 and then increase rapidly. The point on the high Mach number side of the dip were obtained by first bringing the tunnel speed up to about 1.1 Mach number at low dynamic pressure, increasing dynamic pressure at a constant Mach number to a level above the lowest flutter point, and then decreasing Mach number until the flutter boundary was reached. As the dynamic pressure was increased between Mach numbers of 1.00 and 1.05 the wing response changed very gradually from low oscillations to sustained flutter. Consequently, the minimum dynamic pressure at flutter in this region was not precisely defined but lies somewhere in the crosshatched area.

From Figures 11(b) and 12(b) it may be seen that the calculated flutter frequencies are generally in good agreement with measured values both in magnitude and trend with Mach number.

As mentioned previously, the general test procedure was to try to obtain flutter points with a constant nominal lift of 769 Newtons (173 lbf) on each wing (lift at the hypothetical design cruise point). A few test conditions which were repeated with the lift about 50% below the nominal value did not show a significant effect of lift on the flutter condition. The test data were not adequate, however, to show conclusively that the flutter response was completely independent of lift.

The conventional wing was tested with and without transition strips on the upper and lower surfaces to determine what effect, if any, boundary layer tripping might have on the flutter characteristics. No significant effect was noted (Fig. 12). All tests of the supercritical wing were conducted with transition strips.

To study the possibility that the rapid dip in the measured flutter boundaries might be due to tunnel wall interference effects, a 40% size model of the same planform was tested. This wing consisted of an aluminum plate which was covered with balsa to obtain the same airfoil shape as the conventional wing with the same spanwise thickness distribution but with no camber. The node lines and order of frequencies for the first three structural modes were similar to the large wings. The flutter characteristics of the small model were similar to those of the larger wings. It fluttered at a frequency between the first and second natural mode and the flutter boundary exhibited the same rapid decrease near Mach 1 followed by a rapid recovery as was found with the larger wings. It is therefore concluded that the extreme transonic dips exhibited by the larger wings were characteristics of the configurations.

The curves of measured flutter dynamic pressure versus Mach number shown on Figures 11 and 12 are shown again in Figure 13 for direct comparison. At subsonic Mach numbers the boundary for the supercritical wing is above the conventional wing as was predicted by the flutter calculations (reflecting the slight differences in structural properties of the two wings). In the transonic region, however, the supercritical wing boundary decreases more rapidly and the minimum flutter point occurs at a dynamic pressure which is below the conventional wing boundary.

An attempt has been made to adjust the measured results to remove the difference between the boundaries of the two wings due to differences in structural properties. For the calculated flutter points shown in Figure 10, the flutter dynamic pressure ratio, $q_{conventional}/q_{supercritical}$, has an average value of 0.94. In Figure 14 the supercritical wing boundary has been multiplied by 0.94 and is shown for comparison with the unadjusted conventional wing boundary. Thus, when the effects of structural differences are accounted for by use of the subsonic calculated flutter boundaries, it is seen that up to about 0.9 Mach number, the experimental boundaries are almost identical, but the transonic dip is much more pronounced for the supercritical wing.

There are several possible factors which may have caused the minimum flutter dynamic pressure of the supercritical wing to be as much as 30% below that of the conventional wing. It may be that the effects of the slight differences in modal characteristics of the two wings are not completely accounted for in the Mach region from 0.9 to 1.05 by application of a constant factor (based on subsonic calculations) throughout the Mach number range, although it would be difficult to rationalize that the small structural differences alone could account for the difference in the transonic dips shown.

Another possibility is that airfoil shape effects account for some or all of the difference in the flutter boundaries in the sonic range. The nature of these effects have not been definitely ascertained. Unpublished data, obtained from a smaller steel pressure model, also having the same geometry as the F8 supercritical research wing, indicate a 50% to 75% increase in lift-curve-slope at low angles of attack over the Mach number range from about 0.8 to 1.0. The large increase in lift-curve-slope as sonic speed is approached is likely to be an important factor in the relatively sharp transonic dip of both wings since the flutter

dynamic pressure tends to be approximately proportional to the inverse of lift-curve-slope. Unfortunately, no directly comparable lift-curve-slope data are available for the conventional wing used in the current tests so that it is not possible to definitely attribute the more severe transonic dip of the supercritical wing to relatively higher lift-curve-slopes. (Such a comparison will be the subject of a future study.) However, there is some evidence (Ref. 4, for example) to suggest that a supercritical wing designed for optimum aerodynamic characteristics at a high subsonic Mach number can exhibit higher lift-curve-slopes near the design Mach number than a similar wing with conventional airfoil sections.

Another characteristic of the supercritical airfoil that may contribute to the difference in the flutter boundaries is the more "aft loaded" condition of supercritical wings. Chordwise pressure distributions measured on the two wings at the 65% semi-span station showed, as expected, the center of pressure on the supercritical wing to be considerably farther downstream than that of the conventional wing. Unsteady aerodynamic forces acting on the wing due to alternately separating and attaching flow and oscillating shocks therefore may more effectively produce unsteady torsional moments on the supercritical wing.

It should be noted that even if the lower minimum flutter dynamic pressure of the supercritical wing is wholly attributable to airfoil shape effects, the supercritical airfoil shape offers the possibility for greater structural efficiency as a compensating factor. For instance, it should be possible to obtain a stiffer structure for a given structural weight due to the near maximum thickness of the supercritical wing that is maintained over a larger fraction of the chord. In the present study this benefit was not utilized, of course, since the intent was to have the structural stiffnesses of the two wings as nearly the same as possible.

Finally, it should be noted that the results of this study are directly applicable only to the particular high-speed configurations studied. Care should be exercised in applying the results to other supercritical configurations until the mechanisms which produce the observed differences in flutter characteristics are defined.

Concluding Remarks

Experimental and analytical studies to compare the flutter characteristics of a high-speed, transport-type, supercritical wing with those of a nearly structurally identical wing that had conventional airfoil sections indicate the following:

Subsonic kernel function aerodynamic theory predicted very well the flutter boundary of both the supercritical and conventional wings up to about 0.85 Mach number. Analytical results did not indicate the large transonic dip determined experimentally for both wings.

Analytical results indicated that unwanted structural dissimilarities between the two wings had the effect of causing the dynamic pressures at flutter of the conventional wing to be about 94% of those of the supercritical wing.

The natural vibration modes that coalesced to produce flutter were the same for both the supercritical and conventional wings.

No effect of lift on the flutter characteristics of either wing were discernible when lift was reduced by 50%.

Tests on a 40% size simplified model of the conventional wing indicated the same rapid decrease in flutter dynamic pressure and rapid recovery near Mach 1 as was exhibited by the larger models.

With structural dissimilarities accounted for by application of the subsonic analytical results, the flutter boundaries of the supercritical and conventional wings were nearly identical up to a Mach number of about 0.9 after which the supercritical wing experienced a much more pronounced transonic dip.

The results indicate a need for further studies to determine explicitly the aerodynamic mechanisms which contribute to the observed differences in the flutter characteristics of supercritical and conventional wings.

References

[1]Whitcomb, Richard T., "Review of NASA Supercritical Airfoils," ICASE Paper No. 74-10, Presented at the Ninth Congress of the International Council of the Aeronautical Sciences, Haifa, Israel, Aug. 25-30, 1974.

[2]Watkins, Charles E., Runyan, Harry L., Woolston, Donald S., "On the Kernel Function of the Integral Equation Relating the Lift and Downwash Distributions of Oscillating Finite Wings in Subsonic Flow," TR-1234, 1955, NASA.

[3]Desmarais, Robert N., and Bennett, Robert M., "An Automated Procedure for Computing Flutter Eigenvalues," Journal of Aircraft, Vol. 2, No. 6, February 1974, pp. 75-80.

[4]Ayers, Theodore G., "A Wind Tunnel Investigation of the Application of the NASA Supercritical Airfoil to a Variable-Wing-Sweep Fighter Airplane," TM X-2759, July 1973, NASA.

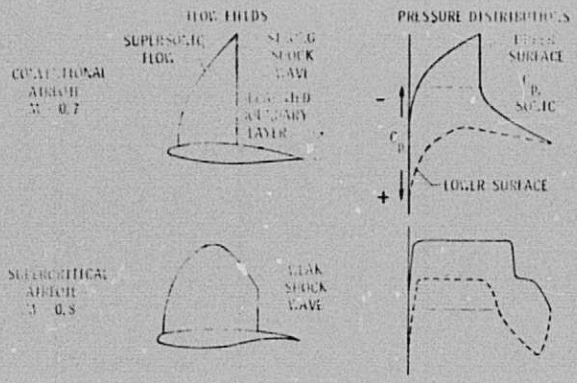

Figure 1. Comparison of supercritical and conventional airfoil static aerodynamic characteristics.

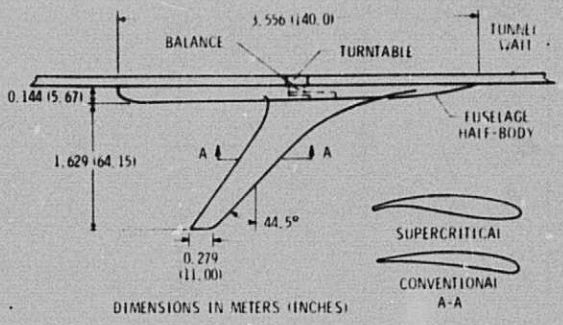

Figure 4. Model geometry.

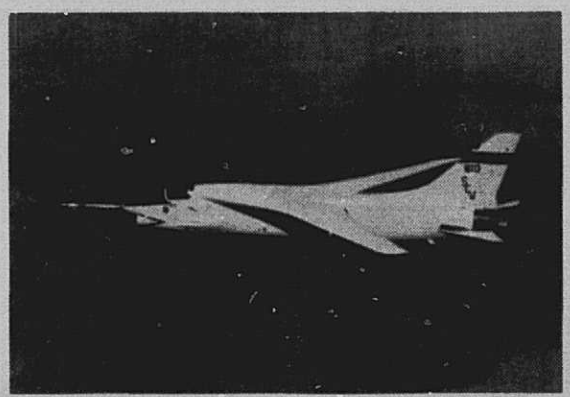

Figure 2. F-8 airplane with transport type supercritical wing in flight.

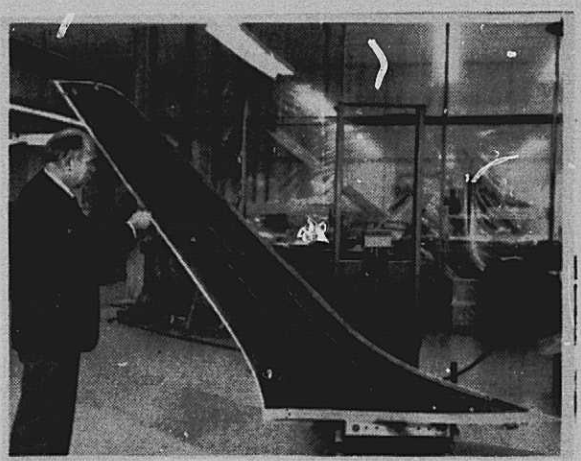

Figure 5. Photograph of supercritical wing panel before bonding of lower surface skin.

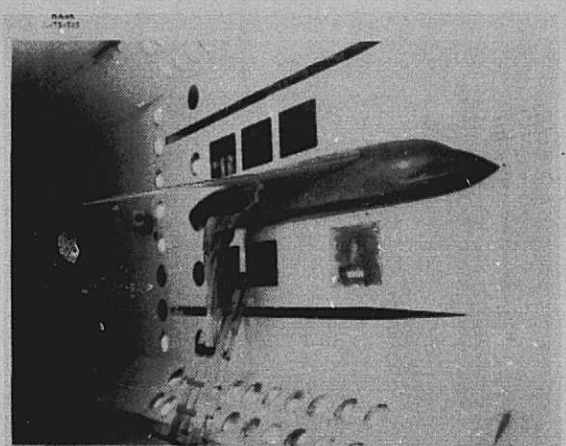

Figure 3. Photograph of supercritical wing model mounted in Langley Transonic Dynamics Tunnel.

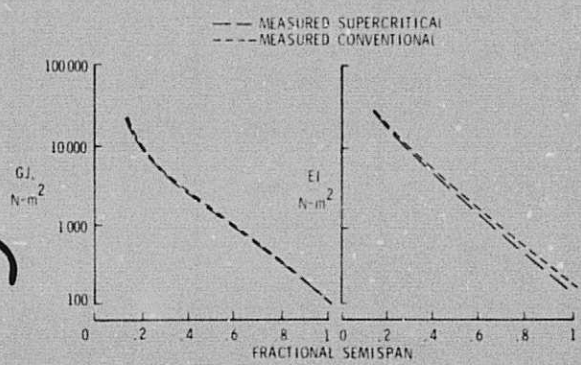

Figure 6. Comparison of stiffness properties.

MODE	SUPERCRITICAL FREQUENCY Hz. NODE LINES	CONVENTIONAL FREQUENCY Hz. NODE LINES
FIRST BEND	5.29	5.47
SECOND BEND	18.08 ———	19.13 — — —
FIRST TORSION	37.10 ———	36.50 ------
THIRD BEND	42.8 — . —	46.0 — . — . —

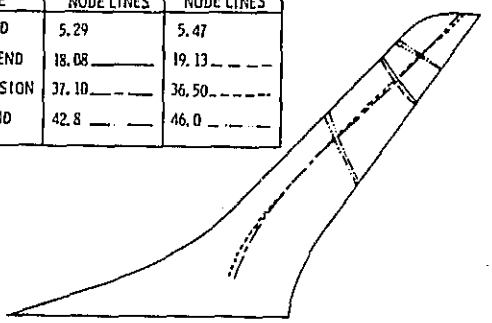

(a) Frequencies and node lines.

MODE	SUPERCRITICAL WING		CONVENTIONAL WING	
	FREQUENCY Hz	GENERAL MASS Kg	FREQUENCY Hz	GENERAL MASS Kg
FIRST BENDING	5.29	.85	5.47	.85
SECOND BENDING	18.08	.47	19.13	.47
FIRST TORSION	37.10	.97	36.50	.92
THIRD BENDING	42.8	.29	46.0	.29

(b) Frequencies and generalized masses.

Figure 7. Comparison of measured natural frequencies, node lines, and generalized masses.

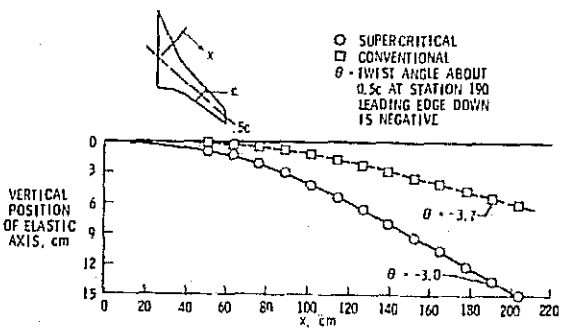

Figure 8. Measured no-wind position of elastic axis ("jig shape").

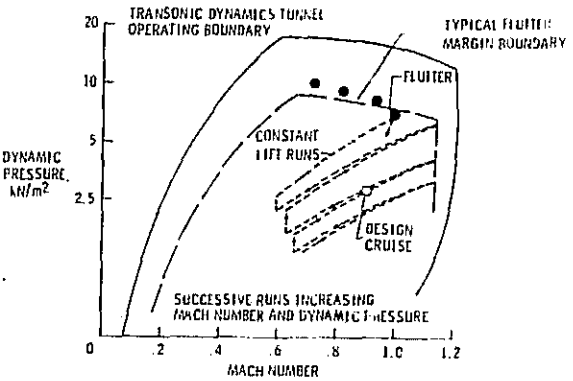

Figure 9. Test procedure for obtaining flutter boundary.

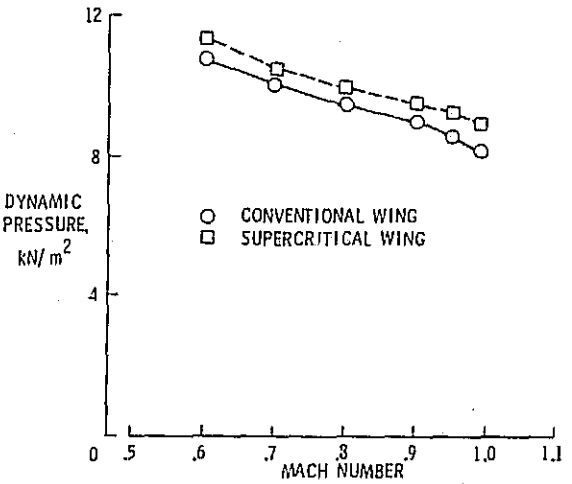

(a) Flutter boundary.

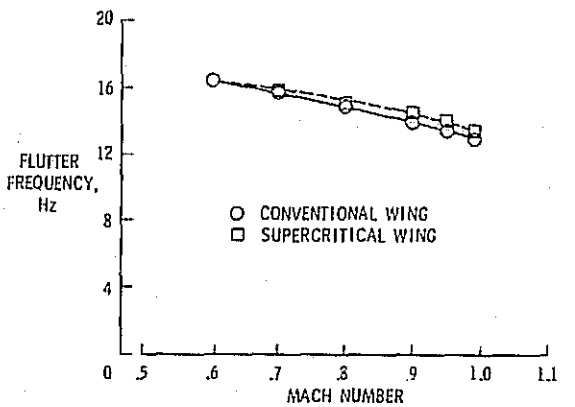

(b) Flutter frequency.

Figure 10. Calculated flutter boundaries and frequencies.

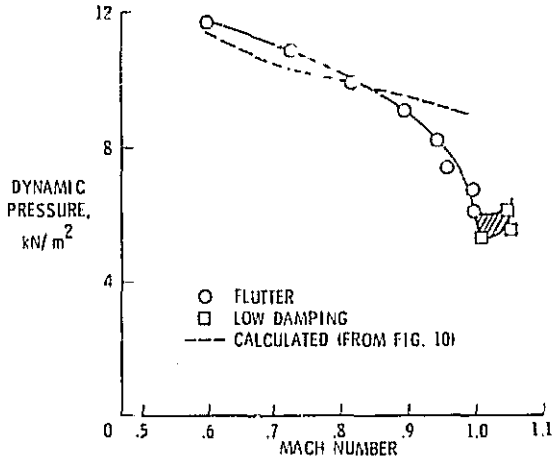

(a) Flutter boundary.

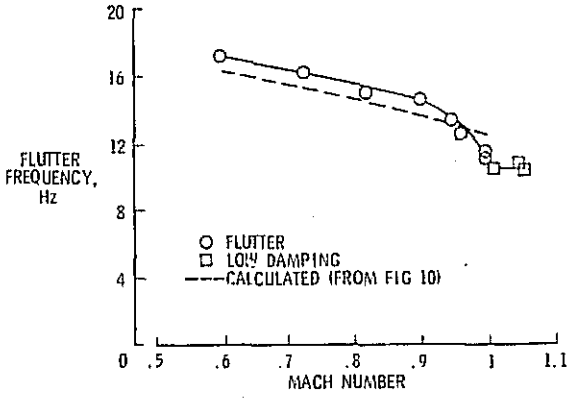

(b) Flutter frequency.

Figure 11. Comparison of measured and calculated flutter characteristics of supercritical wing.

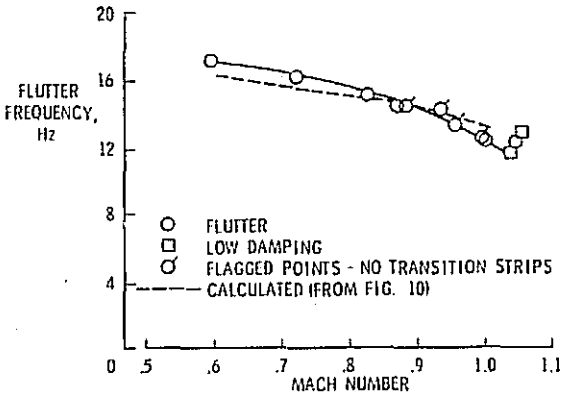

(b) Flutter frequency.

Figure 12. Comparison of measured and calculated flutter characteristics of conventional wing.

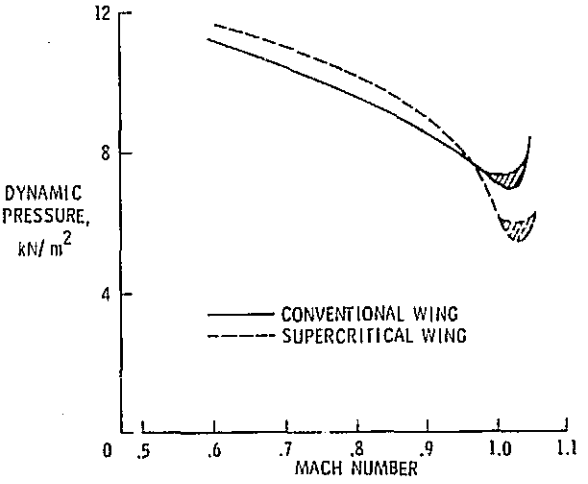

Figure 13. Comparison of measured flutter boundaries of conventional and supercritical wings unadjusted for structural differences.

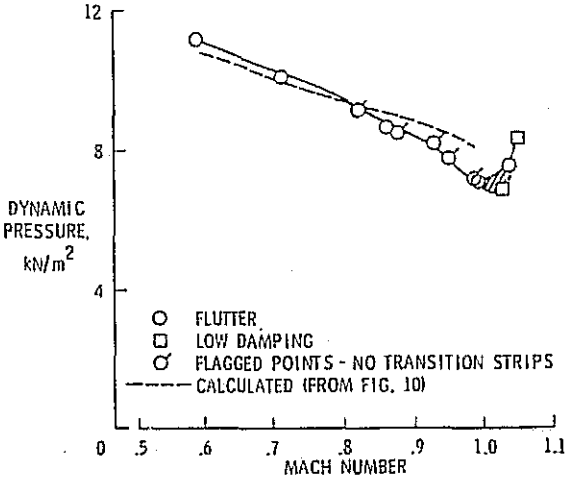

(a) Flutter boundary.

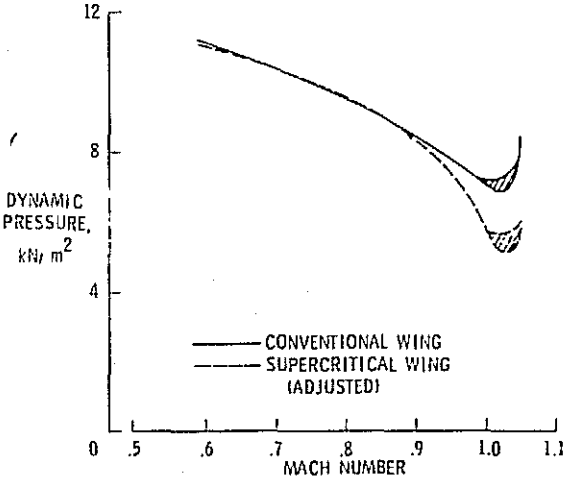

Figure 14. Comparison of conventional wing flutter boundary with adjusted supercritical wing boundary.